Turkish Journal of Chemistry

http://journals.tubitak.gov.tr/chem/

Research Article

Turk J Chem
(2019) 43: 778 – 801

doi:10.3906/kim-1810-60

Effect of Brij 35 and saponin surfactants on adsorption of diethylstilbestrol as an emerging estrogenic contaminant by clinoptilolite in batch and fixed-bed column experiments

Reyhaneh SADDI, Reza FAZAELI*, Leila VAFAJOO, Iraj NASER
Department of Chemical Engineering, Faculty of Engineering, South Tehran Branch, Islamic Azad University, Tehran, Iran

Received: 24.10.2018 • **Accepted/Published Online:** 27.02.2019 • **Final Version:** 11.06.2019

Abstract: In this study, natural clinoptilolite was modified by saponin and Brij 35 surfactants to remove diethylstilbestrol (DES) from wastewater in batch and continuous systems. The optimum pH, amount of adsorbent, contact time, and temperature were 11, 10 g/L, 12 h, and 35 °C, respectively, for the process. The equilibrium data agreed well with the Langmuir isotherm for natural clinoptilolite (NC), natural clinoptilolite modified by Brij 35 (NC-Brij), and natural clinoptilolite modified by saponin surfactants (NC-saponin) compared to other isotherms. The maximum adsorption capacities resulting from the Langmuir isotherm for NC, NC-Brij, and NC-saponin were 8.012, 23.64, and 39.525 mg/g, respectively. Fixed-bed column experiments were performed under various operational conditions to evaluate the performance of the adsorbent bed breakthrough curve. The lumped method solves bed equations to determine the axial dispersion coefficient (D_z) and overall mass transfer coefficient ($K_{overall}$) parameters. Comparison of the kinetic models indicated that the DES adsorption process was well described by the intraparticle diffusion model for NC, pseudo-second-order and fractional power kinetic models for NC-Brij, and pseudo-second-order model for NC-saponin. The negative Gibbs free energy and positive enthalpy changes for NC, NC-Brij, and NC-saponin confirmed that the removal reaction of DES was spontaneous and the adsorption was endothermic, respectively.

Key words: Pharmaceutical contaminant of diethylstilbestrol, saponin and Brij 35 surfactants, natural clinoptilolite, batch and fixed-bed studies

1. Introduction

The extensive presence of pharmaceuticals and steroid hormones in aqueous solutions is nowadays considered an emerging environmental issue.[1] The pharmaceuticals can reach the surface water and groundwater, and, potentially, drinking water, if they are not degraded or removed during sewage treatment.[2] There is considerable concern about personal care products (PPCPs) because of their possible adverse effects on the ecological system and human health. Therefore, it is significant to remove PPCPs from water. Pharmaceuticals such as estrone (E_1), 17bestradiol (E_2), -estriol (E_3), and diethylstilbestrol (DES) are known as natural steroid estrogens.[3] Estrogens are detected at low concentrations usually in ng/L values. Sewage from households, hospitals, the pharmaceutical industry,[4] human activities and industries,[5,6] and wastewater treatment plants[7] has proven to be an important source of discharged pharmaceuticals. Endocrine-disruptive compounds (EDCs) like DES have adverse effects both directly or indirectly, including fertility disorders,[8,9] impaired functioning of the

*Correspondence: r_fazaeli@azad.ac.ir

immune and nervous systems,[10,11] inhibition of normal hormone activities,[12] and sex reversal of males.[13] Two parameters, namely predicted environmental concentration (PEC) and predicted no effect concentration (PNEC), have been considered by the European Medicines Evaluation Authority and Environmental Protection Agency for evaluation of the environmental risks of pharmaceuticals.[14,15] If $0.01 < PEC/PNEC < 0.1$, it is not essential to focus on the hazards of pharmaceuticals. If $0.1 < PEC/PNEC < 1$, the pharmaceutical has insignificant influence. Further, if $1 < PEC/PNEC < 10$, the pharmaceutical has moderate importance. However, if $PEC/PNEC > 10$, the pharmaceutical poses considerable environmental hazards.[16,17] There are many studies and findings about some effective techniques for removal of EDCs from aqueous media consisting of an advanced oxidation process,[18] reverse osmosis,[19] ozonation,[20] filtration membranes,[21] and adsorption.[22] Among the different techniques of removing pharmaceutical contaminants including estrogens and hormones, adsorption is still considered one of the most efficient techniques with a high ratio to remove contaminants as this method is inexpensive, relatively simple, acceptable, widely applicable, and an efficient procedure that produces relatively little sludge. Further, it does not require a high operational temperature.[23,24] Many solid adsorbents have been used for removing pharmaceutical contaminants in the literature such as magnetic particles,[25] fiber membrane,[26] high-silica zeolites,[27] carbonaceous materials,[28,29] and ion exchange resin.[30] Owing to the adsorption efficacy of zeolites, they are considered excellent adsorbents.[31] Natural zeolites are hydrated aluminosilicate minerals with a cage-like structure of tetrahedrons SiO_4 and AlO_4 units composed of water molecules, alkali, and alkaline earth metals in their framework structures.[32] A net negative charge in the structure framework of zeolites, which is due to isomorphic substitution of cations (Si^{+4} and Al^{+3}) in the crystal lattice, can be balanced by exchangeable cations. Therefore, zeolites can be utilized in the sorption of a broad range of organic contaminants with large capacities thanks to their cation-exchange properties.[33,34] Zeolites are widely applied to remove contaminants from wastewater due to their low cost; high availability; size, shape, and charge selectivity; high internal and external surface area; and large cation exchange capacity (CEC) (CEC values ranging from 100 to 200 meq/100 g for natural zeolites and about 450 meq/100 g for synthetic zeolites).[35–38] The zeolite's external surface can be modified by adsorbing nonionic chemical surfactants and biosurfactants. In the present research, Brij 35 was applied as a chemical nonionic surfactant, while saponin was utilized as a natural nonionic surfactant. A surfactant molecule consists of a hydrophilic head and a hydrophobic tail. The head can be composed of an anionic, a cationic, a zwitterion, or a nonionic group, while the tail is a nonpolar hydrocarbon chain.[39] Nonionic surfactants carry no charge and are relatively nontoxic.[40] They are less toxic and have a higher potential for biodegradation than ionic surfactants.[41] In aqueous media at a specific concentration, surfactants form aggregates (concentrations of the critical micelle concentration (CMC)). A micelle is a structure comprising a hydrophilic exterior and a hydrophobic interior acting as a great molecule.[42] At higher concentrations of CMC, surfactants can form other structures. These structures have the potential to constantly form and disintegrate.[43] Surfactants and biosurfactants alter the adsorbent surface properties (adsorbent surface charge) by adsorption onto the adsorbent surface and changing the adsorbent surface hydrophobicity and potential playing significant roles in the interaction of adsorbents with hydrophobic substrates.[44,45] Biosurfactant saponins are glycosides with hydrophilic groups of pentose and hexose and triterpenes like quillaic acid and gypsogenic acid as hydrophobic moieties.[46] Because of the specific molecular structure and superiority with a hydrophilic glycoside backbone and lipophilic triterpene derivative of saponins, they have superior solubilization for hydrophobic organic compounds (HOCs).[47] Brij 35 is polyoxyethylene lauryl ether that is widely applied both in chemical and biochemical processes due to its

advantages including high stability and solubility.[48] Liu et al.[49] investigated the influences of biosurfactants derived from plants such as saponins on the superficial charge of the cell and Cd(II) sorption using *Penicillium simplicissimum*. All the uptake processes, using the intact and saponin-pretreated biomasses, conformed better to the Langmuir isotherm than to the Freundlich equation. The results obtained from the Langmuir isotherm indicated that the maximum adsorption of Cd(II) (q_{max}) was raised by 44.5% when the adsorbent surface was modified with saponin. Esmaeeli et al.[50] evaluated the adsorption of estradiol valerate and progesterone on granular and powdered activated carbon in wastewater. The influences of initial pH of solution, adsorbent dose, temperature, initial concentration of contaminant, and contact time were analyzed. Having examined the kinetic models including pseudo-first-order and pseudo-second-order models, the second-order model had the best agreement with the experimental data. Alvarez-Torrellas et al.[51] compared the sorption performance of tetracycline and ibuprofen from aqueous media using activated carbon from rice husk. The kinetic experimental data were fitted to pseudo-first, pseudo-second, and Elovich kinetic models. The results indicated a great correspondence between the experimental data and the pseudo-second-order model. The equilibrium adsorption data were evaluated by Langmuir, Freundlich, Guggenheim–Anderson–de Boer, Sips, and Temkin adsorption isotherms. Excellent adsorption performances were obtained at the breakthrough time for tetracycline and ibuprofen using activated carbon derived from rice husk via fixed-bed experiments. Dubey et al.[52] utilized developed carbon tubules in order to decontaminate aqueous solutions from three pharmaceutical drugs, i.e. ibuprofen, clofibric acid, and naproxen. The adsorption of the selected pharmaceutical drugs was evaluated in batch and fixed-bed studies. In order to obtain the maximum adsorption capacity and investigate the characteristics of the fixed-bed column, mathematical modeling was used for the experimental data.

To the best of our knowledge, no report has been published on DES sorption on clinoptilolite zeolite modified by Brij 35 and saponin surfactants. Furthermore, no research has compared unmodified clinoptilolite and its forms modified by Brij 35 and saponin with each other in terms of adsorption capacity and adsorption efficiency under different experimental conditions including pH, adsorbent dosage, contact time, and temperature. To date, batch experiments and fixed-bed modeling have not been simultaneously conducted for removal of DES by clinoptilolite. Note that zeolites from different sources have different characteristics, which can affect their adsorption potentials. Accordingly, in this research, natural clinoptilolite was supplied from the Semnan mines in northeastern Iran.

The aim of this study was to modify the surface of natural clinoptilolite by a natural nonionic surfactant (saponin) and a chemical nonionic surfactant (Brij 35) in order to enhance the adsorption capacity of the adsorbent for removal of DES from aqueous media. Furthermore, the removal efficiency of unmodified clinoptilolite and its two forms modified with both surfactants was compared. Moreover, a fixed bed with an upward flow was used in order to remove DES by natural clinoptilolite modified by saponin (NC-saponin) as a better adsorbent compared with the two other forms of the adsorbent (NC and NC modified by Brij 35 (NC-Brij)). The fixed bed column was modeled by the bed equations to predict the breakthrough curve at a specific bed height, flow rate, and DES concentration. The influence of various parameters including pH, contact time, adsorbent dosage, and temperature was evaluated using batch experiments. For modification of the surface of clinoptilolite, different concentrations of Brij 35 and saponin surfactants were prepared in order to determine the surfactant concentration at which the maximum adsorption capacity occurred. Theoretical isotherm models such as Langmuir, Freundlich, and Temkin were compared with the results obtained from batch experiments. Finally, the model parameters were calculated. The experimental data were fitted against pseudo-first-order rate, pseudo-second-order rate, Elovich, liquid film diffusion, intraparticle, and fractional power to interpret the

kinetic data. Eventually, exothermicity or endothermicity and spontaneity and nonspontaneity of the process were found by determining thermodynamic parameters including enthalpy change (ΔH°) and Gibbs free energy change (ΔG°), respectively.

2. Materials and methods

2.1. Materials

The NC used in this study was supplied from the Semnan region in northeast Iran. A raw sample of clinoptilolite was purchased from Afrazand Co. (Tehran, Iran). The nonionic surfactants (saponin and Brij 35) used for preparation of the functionalized clinoptilolite and DES as an adsorbate, which were analytical grade, were provided by Merck. All standard solutions applied during the adsorption experiment were diluted with deionized distilled water. pH adjustments were appropriately performed using 0.1–1 mg/L HNO_3 and NaOH solutions. High performance liquid chromatography (HPLC) (Agilent (Infinity II 1260() was applied to measure the equilibrium concentration of DES. A centrifuge (Kokusan H-200nR) was used to separate solid/liquid phases. pH was measured with a digital pH meter (Satorius PB-11). A vacuum oven (LAB TECH (lvo-2030)) was used for drying the materials in a vacuum. The absorbent was solved in the solution using a shaker (IKA (KS 501 digital). A digital scale was used to weigh the materials (KERN (ALS 220-4)). In order to control the temperature of the room, an accurate temperature controller (Autonics (THD-D)) was used. Regulation of flow rates was done using a peristaltic pump (Etatron DS, Italy) for adjustment of flow rates in the mL/min range.

2.2. Characterization of adsorbent

Table 1 provides the chemical compositions (XRF elemental analysis) of the NC. The surfactants containing C, O, and H in their structures after uptake on the surface of clinoptilolite, due to their low amount, did not significantly change the mass percentage of elements of clinoptilolite. Therefore, only XRF elemental analysis of NC was investigated. However, there was a significant difference in adsorption of DES between modified and unmodified clinoptilolite. The CEC of clinoptilolite was 2.6 meq/g. X-ray diffraction (XRD) was used to analyze the chemical composition of the adsorbent sample. The XRD pattern is shown in Figure 1, which corresponds with the standard reference pattern.

Table 1. Chemical compositions (XRF elemental analysis) of natural clinoptilolite.

Chemical analysis	NC (wt %)
SiO_2	73.26
Al_2O_3	13.6
Na_2O	4.32
K_2O	3.68
CaO	2.52
Fe_2O_3	1.19
MgO	0.91
TiO_2	0.42
P_2O_5	0.07
MnO	0.05

2.3. Preparation of surfactant-modified NC

The modification of NC with Brij 35 was performed by the following procedure. Firstly, NC was washed with boiled deionized water and dried in a furnace at 300 °C for 1 h in order to remove any kind of contaminants on the surface of the adsorbent and to evaporate the water present inside the zeolite pores. Afterwards, the adsorbent was put in a desiccator until its temperature reached the ambient temperature. Accordingly, NC was prepared for surface modification.

2.3.1. Determination of the optimum Brij 35 concentration by modification of the surface of clinoptilolite

In order to modify NC by Brij 35, 50 g of NC was mixed with 1 L of Brij 35 solution in flasks using various concentrations of the surfactant (10, 30, 50, 70, and 90 mg/L). DES concentrations of 1, 20, and 80 mg/L were prepared and then mixed with the above-mentioned concentrations of NC-Brij. Then the flasks were shaken at 180 rpm and 25 °C for 24 h. The mixtures were then filtered and solid samples were dried at 80 °C in an oven for 2 h. The resultant surfactant-modified clinoptilolite was assigned as NC-Brij. Figure 2 illustrates q_e versus C_e at the various concentrations of Brij 35. In the batch experiments, the adsorbent surface was modified by Brij 35 concentration of 50 mg/L. This was because of higher q_e values of the prepared adsorbents with the above surfactant concentration compared to others.

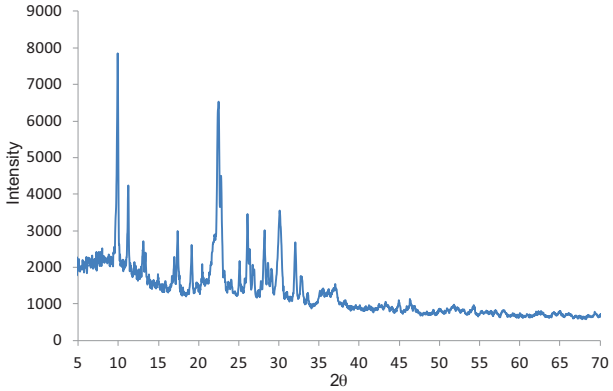

Figure 1. XRD pattern for the natural clinoptilolite.

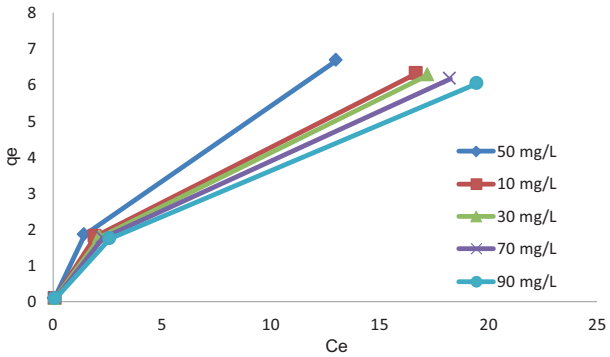

Figure 2. q_e versus C_e in the various concentration of Brij 35.

2.3.2. Determination of the optimum saponin concentration by modification of the surface of clinoptilolite

Modification of the sample with saponin surfactant was performed by the method mentioned in the previous section, with the difference that the surfactant concentrations of 40, 70, 100, 130, and 160 mg/L were investigated. The resulting material was assigned as NC-saponin. Figure 3 demonstrates q_e versus C_e at the various concentrations of saponin. In the batch tests, the adsorbent surface was modified by a saponin concentration of 100 mg/L.

2.4. Modification mechanism of clinoptilolite

The mechanism for DES adsorption on the modified zeolite is coordinate bonding due to the oxygen atoms as the donor and the aluminum as the receiver. Due to the presence of the hydroxide group in Brij 35, there is

the possibility of forming a coordinate bond (dative covalent bond) between the oxygen (Brønsted–Lowry base) and aluminum (Lewis acid) in the clinoptilolite structure. For this reason, surfactant molecules can accumulate on the surface of clinoptilolite. The schematic of the modification mechanism of clinoptilolite with Brij 35 and saponin and all chemical structures are shown in Figure 4.

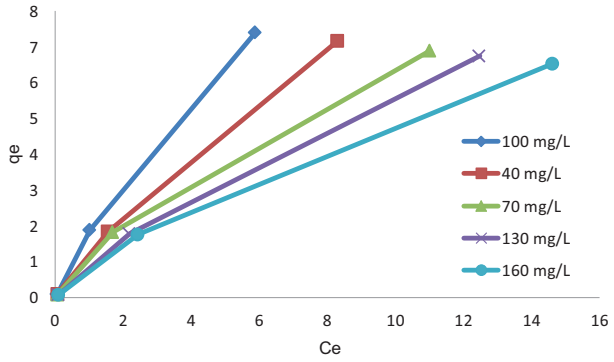

Figure 3. q_e versus C_e in the various concentration of saponin.

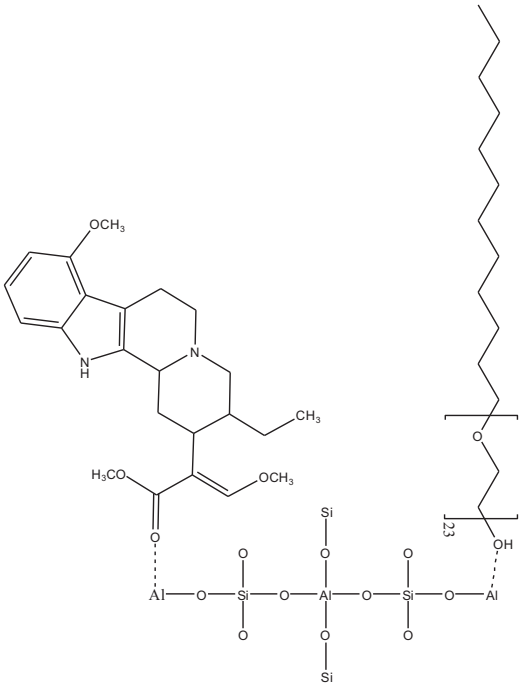

Figure 4. Schematic of the modification mechanism of clinoptilolite with Brij 35 and saponin.

2.5. Batch experiment

Batch tests were conducted across different sets using DES of 0.5–150 mg/L at a fixed dosage (10 g/L) of NC and its two modified forms at pH of 11 and temperature of 35 °C for 12 h. After a time under agitation, the solid–liquid phases were separated by centrifuging at 13,000 rpm for 15 min. The residual DES concentration in a transparent liquid was measured by HPLC analyzer. In chromatograms for sampling at different times, no peak was observed for the surfactants. This proves that no surfactant release takes place during adsorption experiments. Across all batch experiments, a temperature controller was applied for controlling the room temperature. Each experimental effluent concentration determined by HPLC was replicated two or three times, with the average results represented in all figures. The standard deviation range for all experimental data was between 0.09 and 0.17. The removal percentage can be expressed as Eq. (1):[53]

$$R_r\% = \frac{C_0 - C_e}{C_0} \times 100 \tag{1}$$

In order to determine the optimum values of pH, various pH values (2–11) were considered with an initial DES concentration of 0.5 mg/L in contact with 1 g of each form of the adsorbent (NC, NC-Brij, and NC-saponin) at 35 °C for 12 h. The pH at which the surface charge of the adsorbent is zero is called the point of zero charge

pH (pH_{pzc}). The pH_{pzc} of the raw material of the adsorbent and its two modified forms was determined by the following experiment: 0.5 g of the adsorbent was mixed with 100 mL of NaCl 0.1 mg/L solution for 24 h, where the pH of the initial solution was adjusted using HNO_3 and NaOH solution. NaCl solution was used to keep the ionic strength constant. After 24 h, the pH of the solution was measured. Equality of the initial pH of the solution with the pH_{pzc} of the adsorbent proves that the pH is fixed after pouring adsorbent into the solution.[54] In order to measure the minimum time required to reach equilibrium for the unmodified adsorbent and its two modified forms, the samples were shaken from 1 to 24 h in an initial DES concentration of 0.5 mg/L, fixed optimum adsorbent dosage of 10 g/L, pH of 11, and temperature of 35 °C. Furthermore, various kinetic models were evaluated by performing this test in order to determine the kinetic constants. The influence of different doses of NC, NC-Brij, and NC-saponin, ranging from 1 to 10 g/L was examined at constant initial concentration as well as optimum values of pH, temperature, and contact time (12 h). To evaluate the optimum temperature for the three forms of the adsorbent, 5 °C temperature intervals from 20 to 40 °C were used at the constant initial concentration as well as the optimum values of pH, contact time, and adsorbent dosage. Thermodynamic parameters including ΔH°, ΔS°, and ΔG° were calculated upon test analysis.

2.6. Column studies

Due to the higher adsorption performance of NC-saponin compared to NC and NC-Brij across the batch experiments, NC-saponin was used in the fixed-bed column. An upward flow passed through a Pyrex column with a height of 30 cm and diameter of 1 cm. In order to pack spherical particles of NC-saponin in the column, two layers of glass wool were applied at the top and bottom of the fixed bed column. The schema of the experimental setup is illustrated in Figure 5. The operational conditions of the column including the height of 10 cm (equivalent to 15.59 g), DES concentration of 30 mg/L, and flow rate of 10 mL/min were considered in order to study the fixed-bed column. The relationship between the bed height and mass of the adsorbent at the constant column diameter) $\rho_p = \frac{4w}{\pi d_b^2 L}$) determined how to fill the column. For all experiments, the effluent solution was sampled at certain time intervals, with the remaining DES concentration in the solution analyzed by HPLC analyzer. All experiments were performed at 35 °C and pH 11. The maximum adsorption capacity of the adsorbent in a fixed-bed column can be computed using Eqs. (2) and (3):[55]

$$q_{total} = \frac{Q}{1000} \int_0^{t_{total}} (C_0 - C_t)\, dt \tag{2}$$

$$q_{max} = \frac{q_{total}}{w} \tag{3}$$

3. Results and discussion

3.1. Effect of pH

The pH of the aqueous solution is one of the major factors affecting the surface binding sites and the surface charge of the adsorbent.[56] The surface of an adsorbent may be positively or negatively charged depending on the pH_{pzc} value at which no charge is found on the surface. According to Figure 6, the pH_{pzc} values of NC, NC-Brij, and NC-saponin were 8, 8.2, and 8.5, respectively. If $pH_{solution} > pH_{pzc}$, the adsorbent surface is negatively charged and the adsorbent is able to adsorb cations. However, if $pH_{solution} < pH_{pzc}$, the adsorbent surface has a positive charge and the adsorbent allows for adsorption of anions using electrostatic attraction. Figure 7

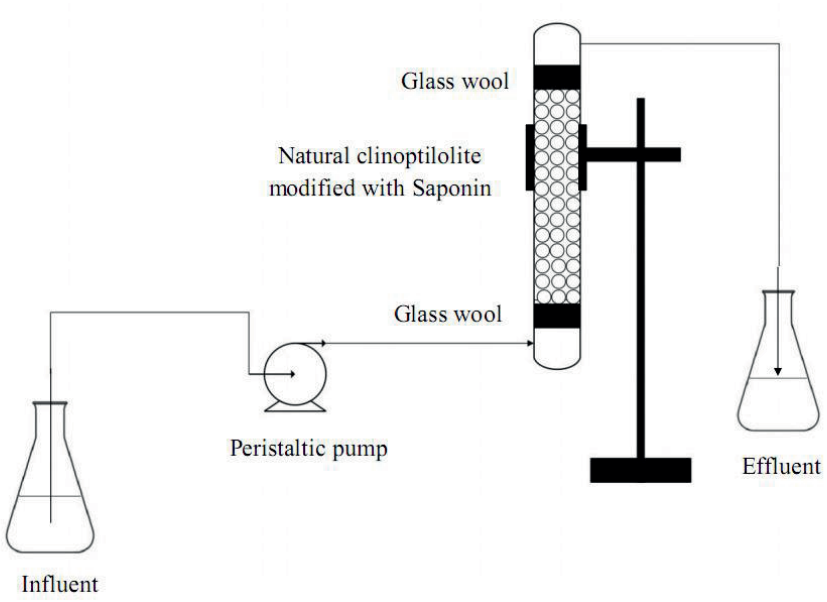

Figure 5. Schematic diagram of the experimental fixed-bed column.

displays the effect of pH within the range of 2–11 on the adsorption of DES from wastewater. DES probably exists as cations when pH $<$ 3.5, as zwitterions at pH range from 3.5 to 7.7, or as anions when pH $>$ 7.7.[57] Generally, the mechanisms of uptake significantly involve electrostatic interaction, hydrogen bonding formation, electron donation–acceptance, and π–π dispersion interaction.[58] Enhanced DES adsorption in highly acidic solutions (pH of 2 to 4) was not related to the electrostatic repulsion between the cationic DES molecules and the positively charged surface of the adsorbent. Accordingly, the uptake was not due to electrostatic interaction. However, the favorable adsorption of DES within the pH values between 2 and 4 could be because of the hydrogen bonding formation.[59] Enhanced removal of the DES from 0.027 to 0.036, 0.031 to 0.04, and 0.04 to 0.043 mg/g and an elevation in the maximum values of removal efficiency of this pharmaceutical contaminant (R_r%) from 54.319% to 73.428%, 63.422% to 80.341%, and 80.605% to 86.714% were obtained by NC, NC-Brij and, NC-saponin adsorbents, respectively, through raising pH from 2 to 4. Then an insignificant change was observed until pH 8. As pH increased from 4 to 8, the molecules of DES existed as zwitterions in the solution. This showed a slight change in DES adsorption. Within the pH range of 8 to 11, elevation in the sorption performance of NC, NC-Brij, and NC-saponin toward DES was obtained from 0.038 mg/g to a maximum of 0.044 mg/g, from 0.041 mg/g to a maximum of 0.046 mg/g, and from 0.043 mg/g to a maximum of 0.047 mg/g (R_r% of 76.726%–88.872%, 83.463%–92.905%, and 87.215%–94.692%), respectively. The major reason for enhanced DES adsorption within the pH interval (8–11) was possibly the $\pi - \pi$ electron donor–acceptor interaction between the adsorbent surface and DES molecule. This kind of interaction represents one of the most significant driving forces for uptake of pharmaceutical contaminants.[60]

3.2. Effect of contact time

The impact of contact time on the amount of DES adsorbed onto NC, NC-Brij, and NC-saponin is exhibited in Figure 8. It is observed that, with an increase in the contact time, the removal efficiency reached its maximum value after 12 h as there are vacant sites at the initial times. However, no significant change in DES uptake

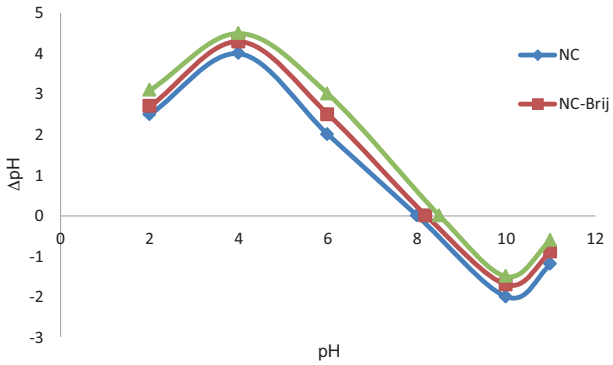

Figure 6. pH_{pzc} of NC, NC-Brij, and NC-saponin.

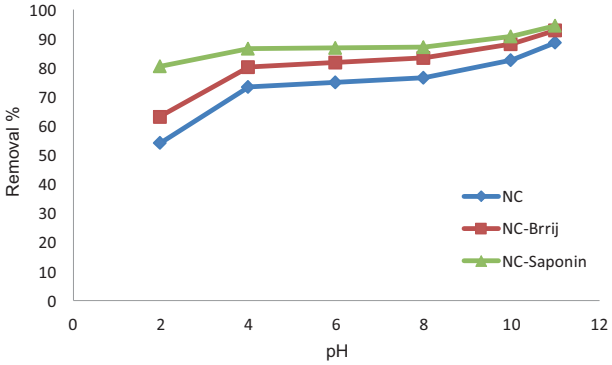

Figure 7. Effect of pH on the diethylstilbestrol removal efficiency.

was seen after 12 h, since the active sites of the adsorbent were saturated by the adsorbate species. At the optimum contact time of 12 h, the maximum values of DES equilibrium adsorption capacity (q_e) were 0.044, 0.046, and 0.047 mg/g for NC, NC-Brij, and NC-saponin, respectively. Moreover, the removal percentages of this pharmaceutical contaminant from aqueous solutions (R_r%) were 88.751%, 92.906%, and 94.982% for NC, NC-Brij, and NC-saponin, respectively.

3.3. Effect of adsorbent level

The effect of the adsorbent dose on the removal of DES is revealed in Figure 9. The results indicated that by raising the adsorbent dosage from 1 to 10 g/L the removal efficiency grew considerably. This is because of greater surface area and increasing accessible sites. The adsorbent dosage at which the maximum removal efficiency occurred was 10 g/L, with the values of removal percentage of this pharmaceutical contaminant obtained as more than 88% for the three forms of the adsorbent. Therefore, all batch experiments were performed at this optimum dosage.

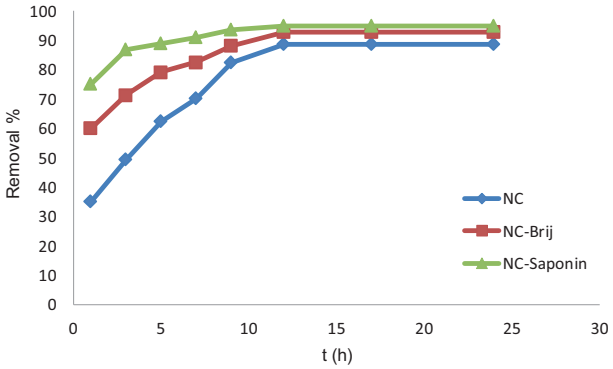

Figure 8. Effect of contact time on the diethylstilbestrol removal efficiency.

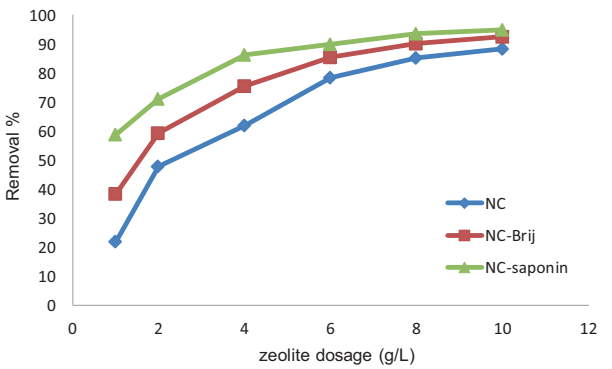

Figure 9. Effect of the adsorbent dosage on the diethylstilbestrol removal efficiency.

3.4. Effect of temperature

The adsorption of DES was performed at five different temperatures (20, 25, 30, 35, and 40 °C) using NC, NC-Brij, and NC-saponin. Figure 10 illustrates the plot of removal percentage versus solution temperature with the

maximum adsorption of DES (R_r % = 80.199, 88.511, and 92.307 and q_e = 0.04, 0.044, and 0.046 mg/g for NC, NC-Brij, and NC-saponin, respectively) at 35 °C. As can be seen, temperature rise resulted in enhanced DES adsorption as the necessary ion exchange activation energy was provided at higher temperatures. Elevated adsorption with temperature elevation up to 35 °C indicated that the adsorption of DES on the adsorbent was an endothermic process. However, after 35 °C, removal efficiency was reduced since the desorption process took place.

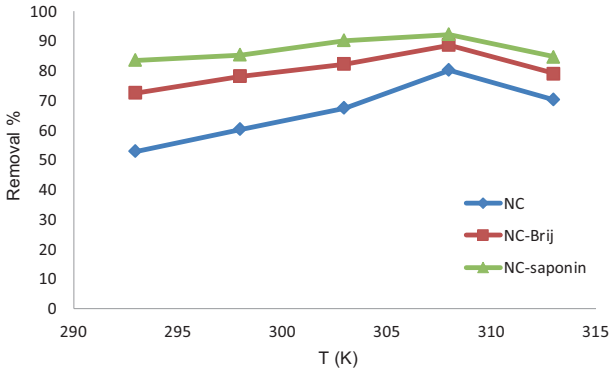

Figure 10. Effect of temperature on the diethylstilbestrol removal efficiency.

3.5. Isotherm model

In order to design and optimize the solid–liquid adsorption process, various isotherm models have been used.[61] In the present research, Langmuir, Freundlich, and Temkin adsorption isotherm models as the most commonly practical isotherms were used to investigate the experimental adsorption equilibrium data in the batch tests. These adsorption isotherm models have been explained in detail by Saadi et al.[62] The linear equations of these three isotherms are reported in Table 2 and the parameters of the isotherm equations are presented in Table 3. The equilibrium adsorption capacity of the adsorbent can be written as Eq. (4).[62]

$$q_e = \frac{V\left(C_o - C_e\right)}{W} \tag{4}$$

Table 2. Adsorption isotherm model equations.

Isotherm model	Equation	Ref.
Langmuir	$\frac{1}{q_e} = \frac{1}{K_L q_{\max}} \frac{1}{C_e} + \frac{1}{q_{\max}}$	79
Freundlich	$\log q_e = \log K_f + \frac{1}{n} \log C_e$	79
Temkin	$q_e = B_T \ln K_T + B_T ln C_e$ $B_T = \frac{RT}{b_T}$	79

3.5.1. Comparison of adsorption isotherm models

The maximum adsorption capacities from the Langmuir isotherm were 8.012, 23.640, and 39.525 mg/g for NC, NC-Brij, and NC-saponin, respectively. These values were obtained from linear regression of $1/q_e$ against $1/C_e$

Table 3. Isotherm model constants.

Isotherm	Parameter	Value (NC)	Value (NC-Brij)	Value (NC-saponin)
Langmuir	q_{max} (mg/g)	8.012	23.640	39.525
	K_L (L/mg)	0.101	0.055	0.047
	R_L	0.951	0.972	0.976
	R^2	1	0.999	1
	MPSD	0.004	0.248	0.005
	χ^2	0.018	0.243	0.040
	ARE	0.045	0.292	0.050
Freundlich	n	1.500	1.444	1.103
	K_f ($mg^{1-n}L^ng^{-1}$)	0.622	1.055	1.628
	R^2	0.940	0.900	0.995
	MPSD	0.136	0.323	0.011
	χ^2	0.123	0.984	0.047
	ARE	0.294	0.425	0.099
Temkin	B_T	1.068	1.381	2.107
	K_T	3.896	6.148	6.346
	R^2	0.914	0.896	0.738
	MPSD	0.179	0.377	0.673
	χ^2	0.255	1.036	0.724
	ARE	0.300	0.448	0.627

(Figure 11). A desirable or undesirable adsorption process in this model can be identified by the dimensionless constant of the separation factor, R_L, which is an equilibrium parameter and calculated by Eq. (5).[62]

$$R_L = \frac{1}{1 + K_L C_0} \tag{5}$$

Favorable, irreversible, and linear adsorption processes are obtained by $0 < R_L < 1$, $R_L = 0$, and $R_L = 1$, respectively.[62] In the present study, the R_L values for the adsorption of DES onto the NC, NC-Brij, and NC-saponin were 0.951, 0.972, and 0.976, respectively, suggesting favorable adsorption onto the three forms of the adsorbent. The plot of the $\log q_e$ against $\log C_e$ (Figure 12) curve for the Freundlich isotherm is a straight line with a slope of $1/n$ and an intercept of $\log K_f$, with n indicating how favorable the adsorption process is. When $n > 1$, $n < 1$, and $n = 1$, these represent favorable, unfavorable, and linear equilibrium adsorption isotherms, respectively.[63] n values revealed that the adsorption process was favorable for NC, NC-Brij, and NC-saponin. B_T and K_T from the Temkin equation can be calculated by drawing the plot of q_e versus $\ln C_e$ (Figure 13).

Linear regression of the isotherm models captures the error between the experimental data and the predicted isotherm. Similarity of the data obtained from the model and experimental data suggests that the

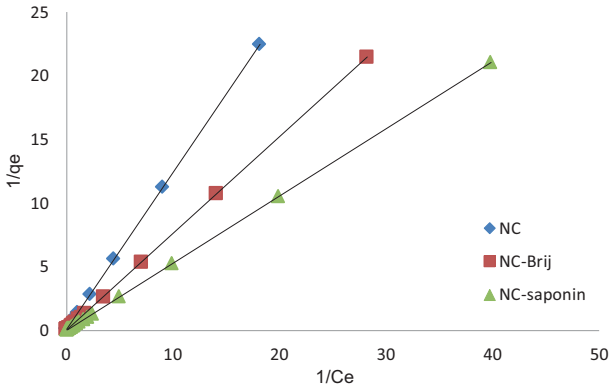

Figure 11. Langmuir plot for adsorption of diethylstilbestrol onto NC, NC-Brij, and NC-saponin.

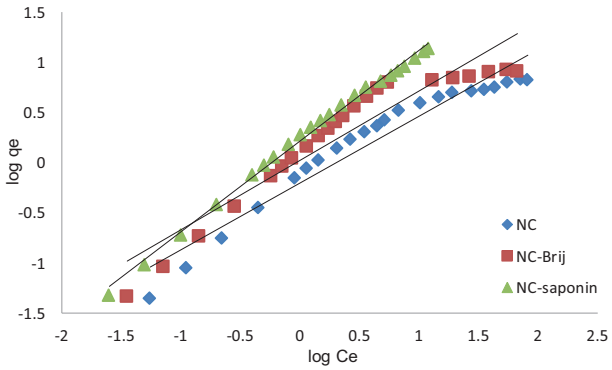

Figure 12. Freundlich plot for adsorption of diethylstilbestrol onto NC, NC-Brij, and NC-saponin.

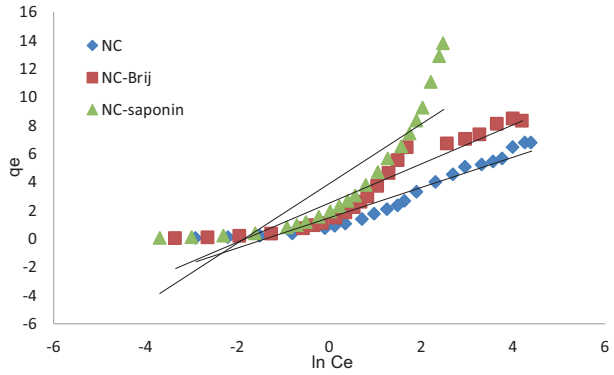

Figure 13. Temkin plot for adsorption of diethylstilbestrol onto NC, NC-Brij, and NC-saponin.

error value would be a small number, while if there is a difference between them, it would be a large number. In the present study, three error functions, Marquardt's percent standard deviation (MPSD),[64] nonlinear chi-square (χ^2),[65] and average relative error (ARE),[64] were studied to determine the fitness of the isotherm equations in relation to the experimental data. The MPSD, χ^2, and ARE functions are given as Eqs. (6), (7), and (8), respectively:

$$\sum_{i=1}^{p}\left(\frac{q_{e,exp}-q_{e,cal}}{q_{e,exp}}\right)_i^2 \quad MPSD \tag{6}$$

$$\sum_{i=1}^{n}\frac{\left(q_{e,exp}-q_{e,cal}\right)^2}{q_{e,cal}} \quad \chi^2 \tag{7}$$

$$\sum_{i=1}^{n}\left|\frac{q_{e,cal}-q_{e,exp}}{q_{e,exp}}\right|_i \quad ARE \tag{8}$$

Note that suitable isotherms for adsorbate sorption by the sorbent are obtained by higher values of correlation coefficient (R^2) and lower values of error function. The values of the correlation coefficients (R^2) and error functions for NC, NC-Brij, and NC-saponin (Table 3), which are adequate criteria for comparing isotherm

models, revealed that the Langmuir isotherm fitted the equilibrium data best. On the other hand, monolayer adsorption of DES on the surface of NC, NC-Brij, and NC-saponin showed that chemisorption occurred for adsorption of DES by the three forms of the adsorbent.

3.6. Column studies

3.6.1. Fixed-bed column modeling

A breakthrough curve, which is a diagram of effluent concentration versus time, is plotted in order to design an adsorbent column. At the initial time, the adsorbate effluent concentration reached its lowest value because there were a number of available sites for the adsorbent, but, over time, the effluent concentration increased due to the occupation of the adsorbent sites by DES. Eventually, the adsorbent bed was saturated as time increased and the effluent concentration reached the influent concentration. In the present study, the bed nonequilibrium model was presented for the overall mass transfer coefficient and pore diffusion mechanism.

Assumptions of the dynamic model of the adsorption process in the experimental conditions are as follows:

- ✓ There was axial dispersion diffusion at the low flow rate.
- ✓ Constant temperature was considered in the low concentration of adsorbate molecules.
- ✓ Concentration gradient existed in the longitudinal direction.
- ✓ The pressure drop was neglected in the liquid phase.
- ✓ Cross section along the bed was constant.
- ✓ Because of the existence of large pores in the adsorbent, surface diffusion was ignored and pore diffusion was assumed.
- ✓ Variations in the rate, fluid, and adsorbed phase concentration in the radial direction were neglected in the fixed bed column.
- ✓ Due to the small adsorbate molecule diameter compared with the adsorbent pore diameter, Knudsen diffusion was neglected and a molecular diffusion mechanism was applied.

According to axial dispersion and pore diffusion resistances controlled by the molecular diffusion mechanism, kinetic adsorption models were presented in this research work. Solution of the partial differential equations (PDEs) was done by the linear method. This method is faster and more accurate than other numerical solution methods because the PDE is converted to an ordinary differential equation (ODE) and only geometric derivatives are expanded. Values for two parameters of the overall mass transfer coefficient ($K_{overall}$) and axial dispersion coefficient (D_z) were determined using the following equations. Breakthrough analysis was studied by a one-dimensional mathematical model for nonequilibrium, isothermal, and axially dispersed single component fixed-bed adsorption.[66] For the adsorbate (component i), partial mass balance with selection of a cylindrical element from a cylindrical bed is presented as Eq. (9) and accumulation is defined as Eq. (10):

$$A\varepsilon uC - A\varepsilon D_z\frac{\partial C}{\partial z} = A\varepsilon\left[uC + \frac{\partial(uC)}{\partial z}dz\right] - A\varepsilon D_z\left[\frac{\partial C}{\partial z} + \frac{\partial^2 C}{\partial z^2}dz\right] + Accumulation \tag{9}$$

$$Accumulation = \varepsilon Adz\frac{\partial c}{\partial t} + \varepsilon_p\frac{\partial c_p}{\partial t}(1-\varepsilon)adz + = \rho_p\frac{\partial q}{\partial t}(1-\varepsilon)adz \tag{10}$$

In Eq. (10), the first, second, and third terms are the bulk fluid accumulation in the element, moderate accumulation of fluid in the pores of the adsorbent in the element, and moderate accumulation of the adsorbent in the element, respectively. Eq. (11) is obtained by rearranging Eqs. (9) and (10):

$$-D_z\frac{\partial^2 C}{\partial z^2}+\frac{\partial(uC)}{\partial z}+\frac{\partial C}{\partial t}+\frac{1-\varepsilon}{\varepsilon}\left[\varepsilon_p\frac{\partial C_p}{\partial t}+\rho_p\frac{\partial q}{\partial t}\right]=0 \tag{11}$$

N_i can be computed by different mass transfer resistances and various formulas. The fluid phase driving force concentration and the solid phase driving force were applied in Eqs. (12) and (13), respectively.[67]

$$N_i=\frac{\partial C_p}{\partial t}\left(\varepsilon_p+\rho_p\frac{\partial q}{\partial C_p}\right)=k_i\left(C-C_p\right) \tag{12}$$

$$N_i=\rho_p\frac{\partial q}{\partial t}=k_i\left(q_e-q\right) \tag{13}$$

Due to the existence of driving force of mass transfer in the solid phase, Eq. (13) was applied in this research study. The initial and boundary conditions are

$$B.C.1: C(z,t)=C_0+\frac{D_z}{u}\frac{\partial C(z,t)}{\partial z}, z=0 \tag{14a}$$

$$B.C.2: \frac{\partial C(z,t)}{\partial z}=0, z=l \tag{14b}$$

$$C(z,0)=0 \tag{14c}$$

Both internal and external mass transfer resistances are added in order to calculate the overall mass transfer coefficient. The overall mass transfer coefficient is presented as Eq. (15).[67]

$$\frac{1}{K_{overall}}=\frac{R_p}{3k_f}+\frac{R_p^2}{15D_p^e\varepsilon_p} \tag{15}$$

The effective pore diffusivity coefficient, D_p^e, and pore diffusivity coefficient, D_p, are computed as Eqs. (16) and (17).[68]

$$D_p^e=\frac{D_p}{\tau_p} \tag{16}$$

$$D_p=\frac{1}{\frac{1}{D_m}+\left(\frac{1}{D_k}\right)} \tag{17}$$

Because the diameter of the adsorbate molecule is smaller than the adsorbent pore diameter, the Knudsen diffusion is negligible. Therefore, Eqs. (16) and (17) are simplified as

$$D_p^e=\frac{D_m}{\tau_p} \tag{18}$$

Because the path of molecule movement into the adsorbent pores is indirect, a tortuosity factor is determined as Eq. (19):[69]

$$\tau_P = \frac{1}{\varepsilon_P} \tag{19}$$

The Sc and Re values are in the range of experimental conditions. Based on agreement with Wakao and Funzakri, the mass transfer coefficient between the fluid and adsorbent particles is written by Eq. (20).[70]

$$sh = \frac{k_f\, d_p}{D_m} = 2 + 1.1\,(Sc)^{0.33}\,(Re)^{0.6} \tag{20}$$

This equation is valid for $0.6 < \ Sc < 70$ and $3 < \ Re < 10{,}000$.

Axial dispersion is assumed for this packed bed since fluid velocity is low. The axial dispersion coefficient is expressed as Eq. (21).[70]

$$\frac{D_z}{D_m} = \gamma_1 + \gamma_2 \frac{dpu}{D_m} = \gamma_1 + \gamma_2 \frac{(Re)\,.\,(Sc)}{\varepsilon} \tag{21}$$

where $\gamma_1 = 20/\varepsilon$ and $\gamma_2 = 0.5$. These values were applied because they had the best agreement with the experimental results.

3.6.2. Breakthrough curve analysis

Figure 14 shows the breakthrough curve for DES sorption from aqueous media at the bed height of 10 cm, flow rate of 10 mL/min, and influent concentration of 30 mg/L. This figure compares theoretical data (solid line) and experimental data (individual points). If the effluent concentration reaches 99% of the influent concentration and effluent concentration reaches 1% of the influent concentration, the bed saturation point and breakthrough point will occur, respectively. With regards to Figure 14, the breakthrough time of 130 min and saturation time of 1290 min were obtained. At different operational conditions, evaluations for experimental and theoretical maximum adsorption capacities of NC-saponin were obtained at 10.792 and 10.427 mg/g, respectively. The parameters of $K_{overall}$ and D_z obtained from the model were calculated as 5.28 $\times 10^{-4}$ 1/s and 3.117 $\times 10^{-4}$ m^2/s, respectively.

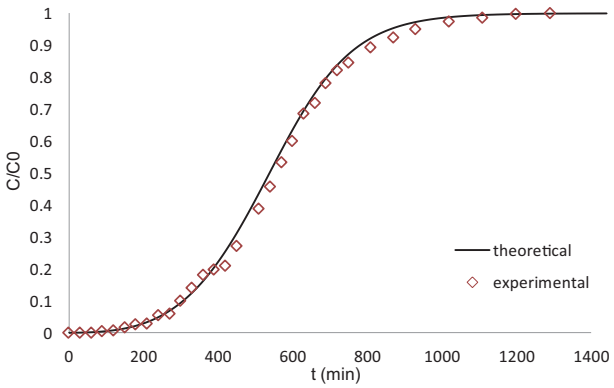

Figure 14. Comparison of experimental breakthrough curves with theoretical in C_0 = 30 mg/L, Q_0 = 10 mL/min, L_0 = 10 cm.

3.7. Kinetic models

The rate controlling mechanism of the adsorption process of DES for the raw clinoptilolite and its modified forms was investigated by six kinetic models. Various kinetic models such as pseudo-first-order rate, pseudo-second-order rate, intraparticle diffusion, Elovich, liquid film diffusion, and fractional power models were considered to fit the experimental data and interpret them. These kinetic models have been discussed in detail by Gupta and Bhattacharyya.[71] The equations of these kinetic models are listed in Table 4 and the parameters of the kinetic models are reported in Table 5.

Table 4. Kinetic model equations.

Kinetic model	Equation	Ref.
Pseudo-first-order rate	$\ln(q_e - q_t) = lnq_e - k_1 t$	72
Pseudo-second-order rate	$\frac{t}{q_t} = \frac{1}{k_2 q_e^2} + \frac{t}{q_e}$ $h = k_2 q_e^2$	73, 74
Intraparticle diffusion	$q_t = k_I t^{1/2} + I$	75
Elovich	$q_t = \frac{1}{\beta}\ln(\alpha\beta) + \frac{1}{\beta} lnt$	76
Liquid film diffusion	$\ln\left(\frac{q_e - q_t}{q_e}\right) = -k_l t + C_L$	77
Fractional power	$lnq_t = lna + blnt$	78

3.8. Comparison of adsorption kinetic models

The plots of $ln(q_e - q_t)$ versus t for the pseudo-first-order rate model, t/q_t versus t for the pseudo-second-order rate model, q_t versus $t^{1/2}$ for the intraparticle diffusion model, q_t versus lnt for the Elovich model, $ln?(\frac{q_e - q_t}{q_e})$ versus t for the liquid film diffusion model, and lnq_t versus lnt for the fractional power model are displayed in Figures 15–20, respectively. In the Elovich model, $\alpha\beta$ is assumed to be more than unity.[79] Moreover, a and b are fractional power model constants where $b < 1$. This model is generally an empirical equation, except when $b = 0.5$.[80] The function ab is also constant, which is the specific sorption rate at t equal to unity.[78] The correlation coefficient (R^2) of the kinetic models for NC, NC-Brij, and NC-saponin are presented in Table 5. According to the table, the high value of R^2 for the DES adsorption on NC indicated that the intraparticle diffusion model was a better fit to the experimental data points than the other kinetic models. Moreover, the adsorption system followed the pseudo-second-order rate and fractional power models better than the other kinetic models for NC-Brij. Furthermore, the adsorption system was well described by the pseudo-second-order rate model for NC-saponin. The q_e value obtained from the pseudo-second-order kinetic model for NC-saponin and NC-Brij was very close to the experimental data.

3.9. Adsorption thermodynamics

The thermodynamic behavior of DES adsorption onto NC, NC-Brij, and NC-saponin was investigated by the thermodynamic parameters at various temperatures including enthalpy change of adsorption (ΔH°), entropy change (ΔS°), and Gibbs free energy change (ΔG°) calculated by Eqs. (22) and (23).[81]

$$\ln K_d = \frac{\Delta S^\circ}{R} - \frac{\Delta H^\circ}{RT} \tag{22}$$

Table 5. Kinetic model parameters.

Kinetic models	Parameter	Value (NC)	Value (NC-Brij)	Value (NC-saponin)
Pseudo-first-order rate model	k_1 (1/h)	3.201	0.229	0.305
	$q_{e,cal}$ (mg/g)	0.040	0.021	0.012
	$q_{e,exp}$ (mg/g)	0.044	0.046	0.047
	R^2	0.920	0.975	0.961
Pseudo-second-order rate model	k_2 (mg/g)	7.846	27.550	63.071
	h	0.019	0.060	0.145
	$q_{e.cal}$ (mg/g)	0.049	0.046	0.048
	$q_{e,exp}$ (mg/g)	0.044	0.046	0.047
	R^2	0.962	0.9959	0.999
Intraparticle diffusion model	k_I (mg/g $h^{1/2}$)	0.011	0.006	0.004
	I	0.005	0.023	0.034
	R^2	0.991	0.992	0.919
Elovich model	α (mg/g h)	0.048	0.746	43.446
	β (g/mg)	97.087	161.290	243.902
	R^2	0.945	0.986	0.977
Liquid film diffusion model	k_l (1/h)	0.252	0.229	0.305
	C_L	-0.087	-0.771	-1.317
	R^2	0.920	0.975	0.961
Fractional power model	a	0.017	0.029	0.038
	b	0.380	0.170	0.097
	R^2	0.987	0.9951	0.970

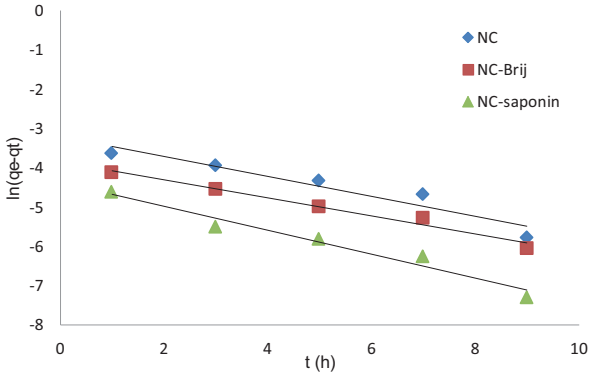

Figure 15. Plot of pseudo-first-order rate model for adsorption of diethylstilbestrol onto NC, NC-Brij, and NC-saponin.

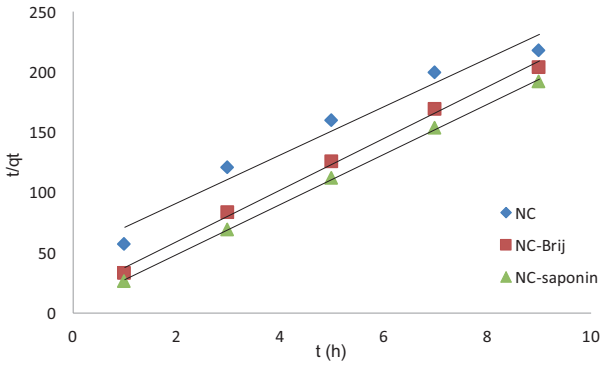

Figure 16. Plot of pseudo-second-order rate model for adsorption of diethylstilbestrol onto NC, NC-Brij, and NC-saponin.

$$\Delta G^\circ = \Delta H^\circ - T\Delta S^\circ = -RT \ln K_d \tag{23}$$

K_d is the distribution coefficient of the sorption process, which is expressed as Eq. (24).[82]

$$K_d = \frac{\rho q_e}{C_e} \tag{24}$$

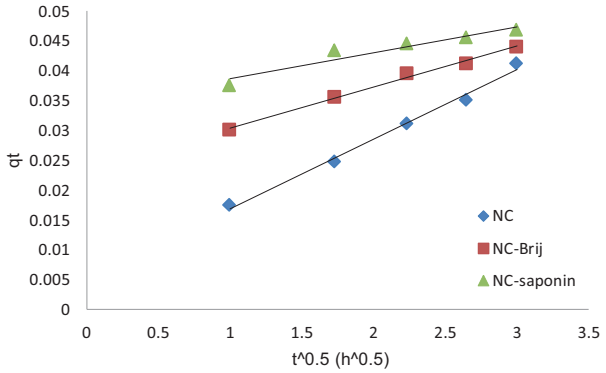

Figure 17. Plot of intraparticle diffusion rate model for adsorption of diethylstilbestrol onto NC, NC-Brij, and NC-saponin.

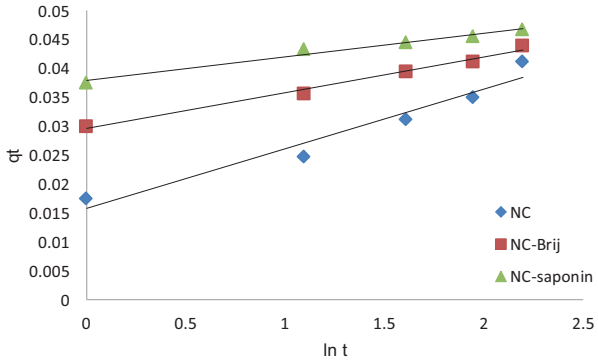

Figure 18. Plot of Elovich rate model for adsorption of diethylstilbestrol onto NC, NC-Brij, and NC-saponin.

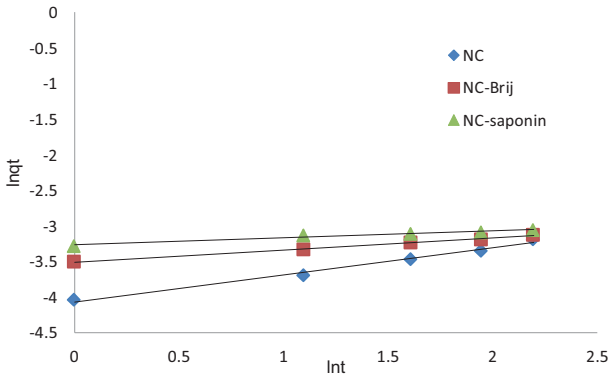

Figure 19. Plot of liquid film diffusion rate model for adsorption of diethylstilbestrol onto NC, NC-Brij, and NC-saponin.

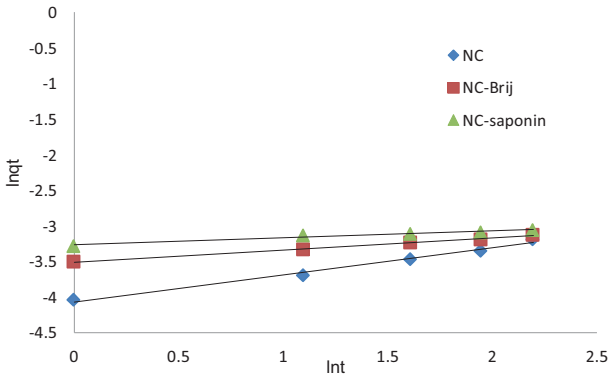

Figure 20. Plot of fractional power rate model for adsorption of diethylstilbestrol onto NC, NC-Brij, and NC-saponin.

The values of ΔH° and ΔS° can be obtained based on the slope and intercept of the plot of $\ln K_d$ against $1/T$, respectively (Figure 21). The corresponding thermodynamic parameters are presented in Table 6. The results (Table 6) suggested that the decline in ΔG° values was caused by temperature rise. Accordingly, the adsorption process is more desirable at higher temperatures. Negative ΔG° values confirmed that the adsorption process is feasible and spontaneous in nature. Furthermore, negative ΔG° revealed the binding energy of DES and solvent. In this regard, this difference between the potential energies of the system components is the driving force of DES molecule redistribution in the system and spontaneous adsorption of DES on the adsorbent.[82] The endothermic process could be attributed to the adsorption of DES onto the clinoptilolite and its two modified forms because of the positive ΔH°, where the removal of the adsorbate was enhanced with temperature elevation.[81] If the enthalpy change of the adsorbent is higher than 40 kJ/mol, chemical sorption takes place. Accordingly, strong electrostatic chemical bonding between the adsorbate and adsorbent surface is concluded. On the other hand, if enthalpy change is less than 20 kJ/mol, the process follows physical sorption.[83,84] In addition, if the adsorption increases with temperature elevation, it suggests that chemical adsorption has taken place. In the present research, the ΔH° values above 40 kJ/mol) 62.287, 51.826, and 45.518 kJ/mol for NC, NC-Brij, and NC-saponin, respectively) and increase in the sorption upon temperature elevation (Figure 10) indicated chemisorption of DES on the three forms of the adsorbent. The positive values of ΔS° indicated

increased randomness at the interface of the adsorbent and adsorbate during the adsorption process.[85] In addition, increased degree of freedom of the adsorbed species was observed due to positive values of ΔS°.[86]

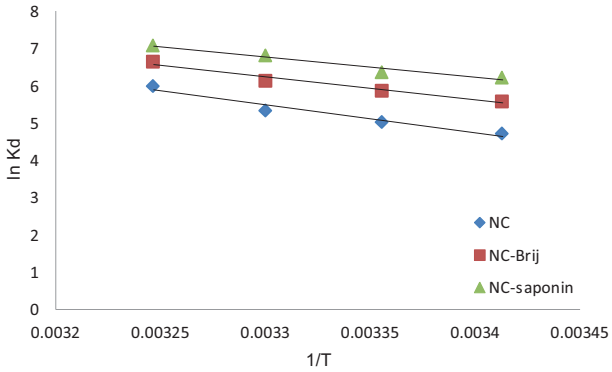

Figure 21. Computation of thermodynamic parameters by the linear plot of $\ln K_d$ versus $1/T$ for adsorption of diethylstilbestrol onto NC, NC-Brij, and NC-saponin.

Table 6. Thermodynamic parameters.

Adsorbent	T (K)	$ln\ (K_d)$	$\boldsymbol{\Delta G^{\circ}(kJ/mol)}$	$\boldsymbol{\Delta H^{\circ}(kJ/mol)}$	$\boldsymbol{\Delta S^{\circ}(J/mol\ K)}$
NC	293	4.718	–11.284	62.287	251.174
	298	5.026	–12.540		
	303	5.333	–13.795		
	308	6.003	–15.051		
NC-Brij	293	5.580	–13.483	51.826	222.939
	298	5.882	–14.598		
	303	6.145	–15.712		
	308	6.646	–16.827		
NC-saponin	293	6.230	–15.015	45.518	206.611
	298	6.360	–16.048		
	303	6.818	–17.081		
	308	7.090	–18.115		

4. Conclusion

Impregnation of NC with Brij 35 and saponin modified the chemical characteristics and surface charge of the adsorbent and presented a good potential sorbent for removal of DES from aqueous solutions. XRD analysis was used for the characterization of clinoptilolite and its two modified forms. The adsorption process is considerably dependent on solution pH, contact time, adsorbent dosage, and temperature. In the present study, the removal efficiency of DES grew as pH increased from 2 to 4 and slightly changed from 4 to 8. Afterwards, it rose up to a pH of 11. Accordingly, the maximum removal percentages (88.872%, 92.905%, and 94.692% for NC, NC-Brij, and NC-saponin, respectively) and maximum equilibrium adsorption capacities of the adsorbents (0.044, 0.046, and 0.047 mg/g for NC, NC-Brij, and NC-saponin, respectively) were obtained at the optimum pH of 11. The pH_{pzc} values were 8, 8.2, and 8.5 for NC, NC-Brij, and NC-saponin, respectively. The results indicated that

the removal efficiency improved with increasing contact time, adsorbent dosage, and temperature from 1 to 12 h because of increased contact of DES with the adsorbent; from 1 to 10 g/L because of greater surface area and more accessible sites; and from 20 to 35 °C, respectively. The optimum contact time, adsorbent dosage, and temperature were determined as 12 h, 10 g/L, and 35 °C, respectively. Based on high values of correlation coefficients (R^2) and the minimum relative errors (MPSD, χ^2, and ARE) for the Langmuir, Freundlich and Temkin isotherms, the Langmuir isotherm matched well the adsorption equilibrium data of DES from wastewater on NC and its two modified forms NC-Brij and NC-saponin. The order of isotherm models based on the model agreement with the experimental data for NC, NC-Brij, and NC-saponin was Langmuir > Freundlich > Temkin. The values of maximum removal efficiency ($q_{\max}$) of NC, NC-Brij, and NC-saponin resulting from the Langmuir isotherm were 8.012, 23.64, and 39.525 mg/g, respectively, by the Langmuir isotherm. The maximum removal efficiency of DES from water using NC-saponin was 4.9 and 1.6 times higher than that of NC and NC-Brij, respectively. Therefore, of the two surfactants tested for modification of clinoptilolite, NC-saponin showed a remarkable potential to remove DES from aqueous solutions. Dimensionless constants of separation factor (R_L) between zero and one (R_L = 0.951, 0.972, and 0.976 for NC, NC-Brij, and NC-saponin, respectively) suggested that the process of DES sorption by all three forms of the adsorbent was favorable. The adsorption capacity of the adsorbent and shape of the breakthrough curve were influenced by three parameters: the initial DES concentration, flow rate, and bed height. Partial mass balance along the bed in the lumped method can explain the behavior of the breakthrough curve for removal of DES onto NC-saponin in a fixed-bed column. The surface diffusion, pore diffusion, and axial dispersion diffusion resistances were considered in the model. On the other hand, surface diffusion resistance was not considered as this resistance was negligible. The model parameters, consisting of the overall mass transfer coefficient ($K_{overall}$) and axial dispersion coefficient (D_z) were obtained as 5.28 $\times 10^{-4}$ 1/s and $3.117 \times 10^{-4} m^2$/s, respectively, under operational conditions of bed height of 10 cm, initial DES concentration of 30 mg/L, and flow rate of 10 mL/min by fitting the experimental data to the theoretical model. Under the aforementioned conditions, evaluations for experimental and theoretical maximum adsorption capacities of NC-saponin were 10.792 and 10.427 mg/g, respectively. Based on the breakthrough curve, the saturation point of 1290 min and breakthrough point of 130 min resulted. In the kinetic study, different models including pseudo-first-order rate, pseudo-second-order rate, Elovich, liquid film diffusion, intraparticle diffusion, and fractional power were evaluated. The findings suggested that for NC the intraparticle diffusion kinetic model, for NC-Brij the pseudo-second-order rate model as well as the fractional power model, and for NC-saponin the pseudo-second-order rate model were the best choices among all the investigated kinetic models to predict the adsorption behavior of DES onto clinoptilolite and its two modified forms. The thermodynamic parameters including enthalpy change of adsorption (ΔH°), entropy change (ΔS°), and Gibbs free energy change (ΔG°) were calculated at various temperatures (20, 25, 30, and 35 °C). The negative values of Gibbs free energy of adsorption confirmed that the process was spontaneous. Moreover, the decline in the values of ΔG° with temperature rise yielded greater DES adsorption at higher temperatures. Furthermore, due to the positive values of enthalpy, the sorption was an endothermic process. Chemisorption was observed for DES adsorption on NC, NC-Brij, and NC-saponin, as the enthalpy change of the adsorbent was higher than 40 kJ/mol for the three forms of the adsorbent and there was an increase in the adsorption with temperature rise. The positive values of ΔS° indicated increased randomness at the interface of the adsorbent and adsorbate during the adsorption. Finally, enhanced degree of freedom of adsorbed species was observed due to positive values of ΔS°.

Nomenclature

a	Fractional power constant
A	Cross-section area of bed (m^2)
b	Fractional power constant
b_T	Temkin constant related to heat of sorption (L/mg)
B_T	Temkin empirical isotherm constant
C	Bulk concentration (mg/L)
C_0	Initial concentration of pharmaceutical contaminant (mg/L)
C_e	Equilibrium concentration of pharmaceutical contaminant (mg/L)
C_L	Intercept of liquid film diffusion model
C_p	Pore concentration (mg/L)
C_t	Concentration in specified time (mg/L)
D_k	Knudsen diffusion coefficient (m^2/s)
D_m	Molecular diffusion coefficient (m^2/s)
d_p	Diameter of adsorbent particle (m)
D_p	Pore diffusivity coefficient (m^2/s)
D_p^e	Effective pore diffusivity coefficient (m^2/s)
D_z	Axial dispersion coefficient (m^2/s)
h	Initial adsorption rate in pseudo-second-order rate model
I	Intercept of intraparticle diffusion model related to the thickness of boundary layer
k_1	Rate constant for pseudo-first-order rate model (1/h)
k_2	Rate constant for pseudo-second-order rate model (g/mg h)
K_d	Distribution coefficient of sorption process
k_f	External mass transfer coefficient (m/s)
K_f	Freundlich constant correlated to adsorption capacity (mg^{1-n} $L^n g^{-1}$)
k_i	Lumped mass transfer coefficient
k_I	Intraparticle diffusion rate constant (mg/g $h^{1/2}$)
k_l	Liquid film diffusion rate constant, which is the external mass transfer coefficient (1/h)
K_L	Langmuir constant related to the free energy of adsorption
$K_{overall}$	Overall mass transfer coefficient (1/s)
K_T	Temkin empirical isotherm constant
L	Bed height (m)
n	Freundlich constant correlated to adsorption intensity
N_i	Mass transfer flux (mol/L s)
q	Solid concentration (mg/g)
Q	Flow rate (mL/min)
q_e	Amount of pharmaceutical contaminant at equilibrium time or equilibrium adsorption capacity of adsorbent (mg/g)
$q_{e,cal}$	Theoretical equilibrium adsorption capacity of adsorbent (mg/g)
$q_{e,exp}$	Experimental equilibrium adsorption capacity of adsorbent (mg/g)
$q_{\max}$	Maximum adsorption capacity of adsorbent (mg/g)
q_t	Amounts of pharmaceutical contaminant at time t (mg/g)
R	Universal gas constant, 8.314 (J/mol K)
R_L	Dimensionless constant of the separation factor

R_p	Radius of adsorbent particle (m)
R_r	Removal percentage of pharmaceutical contaminant from aqueous solution
Re	Reynolds dimensional number
Sc	Schmidt dimensional number
t	Time (h)
T	Adsorption absolute temperature (K)
u	Fluid velocity (m/s)
V	Volume of pharmaceutical contaminant solution (L)
w	Weight of adsorbent (g)

Greek Letters

$\boldsymbol{\alpha}$	Elovich initial adsorption rate constant related to chemisorption rate (mg/g h)
$\boldsymbol{\beta}$	Elovich rate constant related to surface coverage (g/mg)
$\boldsymbol{\Delta G^\circ}$	Gibbs free energy change (kJ/mol)
$\boldsymbol{\Delta H^\circ}$	Enthalpy of adsorption (kJ/mol)
$\boldsymbol{\Delta S^\circ}$	Entropy change (J/mol K)
$\boldsymbol{\varepsilon}$	Intraparticle void fraction of bed
$\boldsymbol{\varepsilon_p}$	Adsorbent porosity
$\boldsymbol{\tau_p}$	Tortuosity factor
$\boldsymbol{\rho}$	Density of water (g/L)
$\boldsymbol{\rho_p}$	Adsorbent particle density (mg/L)

References

1. Yu, Y.; Huang, Q.; Wang, Z.; Zhang, K.; Tang, C.; Cui, J.; Feng, J.; Peng, X. *J Environ. Monit.* **2011**, *13*, 871-878.
2. Hartmann, J.; Beyer, R.; Harm, S. *Environ. Process.* **2014**, *1*, 87-94.
3. D'Ascenzo, G.; Di, Corcia A.; Gentili, A.; Mancini, R.; Mastropasqua, R.; Nazzari, M.; Samperi, R. *Sci. Total Environ.* **2003**, *302*, 199-209.
4. Verlicchi, P.; AlAukidy, M.; Zambello, E. *Sci. Total. Environ.* **2012**, *429*, 123-155.
5. Gavrilescu, M.; Demnerova, K.; Aamand. J.; Agathos, S.; Fava, F. *New Biotechnol.* **2015**, *32*, 147-156.
6. Firouzbakht, S.; Gitipour, S.; Rooz, A. F. H. *Int. J. Environ. Res.* **2017**, 11, 439-448.
7. Kimura, K.; Hara, H.; Watanabe, Y. *Environ. Sci. Technol.* **2007**, *41*, 3708-3714.
8. Diamantikandarakis, E.;, Bourguignon, J. P.; Giudice, L. C.; Hauser, R.; Prins, G. S.; Soto, A. M.; Zoeller, R. T.; Gore, A. C. *Endocr. Rev.* **2009**, *30*, 293-342.
9. Han, B.; Zhang, M.; Zhao, D.; Feng, Y. *Water. Res.* **2015**, *70*, 288-299.
10. Racz, L.; Goel, R. K. *J. Environ. Monit.* **2010**, *12*, 58-70.
11. Sumpter, J. P.; Jobling, S. *Environ. Toxicol. Chem.* **2013**, *32*, 249-251.
12. Roepkea, T. A.; Snyder, M. J.; Cherr, G. N. *Aqua. Toxicol.* **2005**, *71*, 155-173.
13. Jiang, L.; Liu, Y.; Zeng, G.; Liu, S.; Hu, X.; Zhou, L.; Tan, X.; Liu, N.; Li, M.; Wen, J. *Chem. Eng. J.* **2018**, *339*, 296-302.
14. Jones, O. A. H.; Voulvoulis, N.; Lester, J. N. *Water. Res.* **2002**, *36*, 5013-5022.

15. Sebastine, I. M.; Wakeman, R. J. *IChemE.* **2003**, *81*, 229-235.
16. Mihciokur, H.; Oguz, M. *Environ. Toxicol. Pharm.* **20st**, *46*, 174-182.
17. Stockholm County Council 2012 Environmentally Classified Pharmaceuticals Report.
18. Klavarioti, M.; Mantzavinos, D.; Kassinos, D. *Environ. Int.* **2009**, *35*, 402-417.
19. Gur-Reznik, S.; Katz, I.; Dosoretz, C. G. *Water. Res.* **2008**, *42*, 1595-1605.
20. Maniero, M. G.; Bila, D. M.; Dezotti, M. *Sci.Total Environ.* **2008**, *407*, 105-115.
21. Heo, J.; Flora, J. R. V.; Her, N.; Park, Y.; Cho, J.; Son, A.; Yoon, Y. *Sep. Purif. Technol.* **2012**, *90*, 39-52.
22. Ahmed, M. B.; Zhou, J. L.; Ngo, H .H.; Guo, W.; Chen, M. *Bioresour. Technol.* **2016**, *214*, 836-851.
23. Kannan, N.; Rengasamy, G. *Water. Air. Soil. Pollut.* **2005**, *163*, 185-201.
24. Jiang, L. H.; Liu, Y. G.; Zeng, G. M.; Xiao, F. Y.; Hu, X. J.; Hu, X.; Wang, H.; Li, T. T.; Zhou, L.; Tan, X. F. *Chem. Eng. J.* **2016**, *284*, 93-102.
25. Alvarez, P. M.; Jaramillo, J.; Lopez-Pinero, F.; Plucinski, P. K. *Appl. Catal. B Environ.* **2010**, *100*, 338-345.
26. Chang, S.; Waite, T. D.; Schafer, A. I.; Fane, A. G. *Desalination* **2002**, *146*, 381-386.
27. Rossner, A.; Snyder, S. A.; Knappe, D. R. U. *Water. Res.* **2009**, *43*, 3787-3796.
28. Jung, C.; Son, A.; Her, N.; Zoh, K. D.; Cho, J.; Yoon, Y. *J. Ind. Eng. Chem.* **2015**, *27*, 1-11.
29. Reynel-Avila, H. E.; Mendoza-Castillo, D. I.; Bonilla-Petriciolet, A.; Silvestre-Albero, J. *J. Mol. Liq.* **2015**, *209*, 187-195.
30. Zhang, Y.; Zhou, J. L. *Water. Res.* **2005**, *39*, 3991-3991.
31. Braschi, I.; Blasioli, S.; Buscaroli, E.; Montecchio, D.; Martucci, A. *J. Environ. Sci.* **2016**, *43*, 302-312.
32. Lin, J.; Zhan, Y.; Zhu, Z.; Xing, Y. *J. Hazard. Mater.* **2011**, *193*, 102-111.
33. Sun, K.; Shi, Y.; Xu, W.; Potter, N.; Li, Z.; Zhu, J. *Chem. Eng. J.* **2017**, *313*, 336-344.
34. Guo, Y.; Huang, W.; Chen, B.; Zhao, Y.; Liu, D.; Sun, Y.; Gong, B. *J. Hazard. Mater.* **2017**, *339*, 22-32.
35. Yang, X.; Yang, S.; Yang, S.; Hu, J.; Tan, X.; Wang, X. *Chem. Eng. J.* **2011**, *168*, 86-93.
36. Bosch, P.; Olguin, M. T.; Bulbulian, S. Zeolitas naturales, características, propiedades y usos. Universidad Nacional Autonoma de Mexico. P. 192.
37. Kragovic, M.; Dakovic, A.; Sekulic, Z.; Trgo, M.; Ugrina, M.; Peric, J.; Gatta, G. D. *Appl. Surf. Sci.* **2012**, *258*, 3667-3673.
38. Hernandez-Morales, V.; Nava, R.; Acosta-Silva, Y. J.; Macías-Sánchez, S. A.; Pérez-Buenom, J. J.; Pawele, B. *Micropor. Mesopor. Mater.* **2012**, *160*, 133-142.
39. Azarmi, R.; Ashjaran, A. *J. Chem. Pharm. Res.* **2015**, *7*, 632-640.
40. Kumar, G. P.; Rajeshwarrao, P. *Acta. Pharmaceutica. Sinica B* **2011**, *1*, 208-219.
41. Zhuang, G.; Zhang, Z.; Wu, H.; Zhang, H.; Zhang, X.; Liao, L. *Colloids and Surfaces A: Physicochem. Eng. Aspects.* **2017**, *518*, 116-123.
42. Nivas, B. T.; Sabatini, D. A.; Shiau, B. J.; Harwell, J. H. *Water. Res.* **1996**, *30*, 511-520.
43. Rosen, M. J. *Surfactants and Interfacial Phenomena*; Wiley: Hoboken, NJ, USA, 2004.
44. Zhong, H.; Zeng, G. M.; Liu, J. X.; Xu, X. M.; Yuan, X. Z.; Fu, H. Y.; Huang, G. H.; Liu, Z. F.; Ding, Y. *Appl. Microbiol. Biotechnol.* **2008**, *79*, 671-677.
45. Kaczorek, E.; Urbanowicz, M.; Olszanowski, A. *Colloids Surf. B: Biointerfaces* **2010**, *81*, 363-368.
46. Pijanowska, A.; Kaczorek, E.; Chrzanowski, L.; Olszanowski, A. *World J. Microbiol. Biotechnol.* **2007**, *23*, 677-682.
47. Kobayashi, T.; Kaminaga, H.; Navarro, R. R.; Iimura, Y. *J. Environ Sci. Health, Part A* **2012**, *47*, 1138-1145.
48. Cheng, L. *Handbook of Surfactant Application*; Beijing Polytechnic University Press: Beijing, China, 1994.

49. Liu, Z. F.; Zeng, G. M.; Zhong, H.; Yuan, X. Z.; Jiang, L. L.; Fu, H. Y.; Ma, X. L.; Zhang, J. C.; **2011**, *86*, 364-369.
50. Esmaeeli, F.; Gorbanian, S. A.; Moazez, N.; *Int. J. Environ. Res.* **2017**, 11, 695-705.
51. Alvarez-Torrellas, S.; Rodríguez, A.; Ovejero, G.; García, J. *Chem. Eng. J.* **2016**, *283*, 936-947.
52. Dubey, S. P.; Dwivedi, A. D; Lee, C.; Kwon, Y. N.; Sillanpaa, M.; Ma, L. Q. *J. Ind. Eng. Chem.* **2014**, *20*, 1126-1113.
53. Afkhami, A.; Tehrani, M. S.; Bagheri, H. *J. Hazard. Mater.* **2010**, *181*, 836-851.
54. Dastgheib, S. A. Rockstraw, D. A. *Carbon* **2002**, *40*, 843-851.
55. Unuabonah, E. I.; El-Khaiary, M. I.; Olu-Owolabi, B. I. *Chem. Eng. Res. Design.* **2012**, *90*, 1105-1115.
56. Sharma, Y. C.; Srivastava, V.; Mukherjee, A. K. *J. Chem. Eng. Data* **2010**, *55*, 2390-2398.
57. Zhang, X.; Bai, B.; Puma, G. L.; Wang, H.; Suo, Y. *Chem. Eng. J.* **2016**, *284*, 698-707.
58. Martins, A. C.; Pezoti, O.; Cazetta, A. L.; Bedin, K. C.; Yamazaki, D. A. S.; Bandoch, F. G.; Asefa, T.; Visentainer, J. V.; Almeida, V. C. *Chem. Eng. J.* **2015**, *260*, 291-299.
59. Zhang, D.; Yin, J.; Zhao, J.; Zhu, H.; Wang, C. *J. Environ. Chem. Eng.* **2015**, *3*, 1504-1512.
60. Marzbali, M. H.; Esmaieli, M.; Abolghasemi, H.; Marzbali, M. H. *Process. Saf. Environ.* **2016**, *102*, 700-709.
61. Belviso, C.; Cavalcante, F.; Lettino, A.; Fiore, S. *Appl. Clay Sci.* **2013**, *80*, 162-168.
62. Saadi, R.; Saadi, Z.; Fazaeli, R.; Elmi Fard, N. *Korean J. Chem. Eng.* **2015**, *32*, 787-799.
63. Fytianos, K.; Voudrias, E.; Kokkalis, E. *Chemosphere* **2000**, *40*, 3-6.
64. Ho, S.; Porter, J. F.; Mckay, G. *Water. Air. Soil. Poll.* **2002**, *141*, 1-33.
65. Boulinguiez, B.; Le Cloirec, P.; Wolbert, D. *Langmuir* **2008**, *24*, 6420-6424.
66. Ghorai, S.; Pant, K. K. *Chem. Eng. J.* **2004**, *98*, 165-173.
67. Siahpoosh, M.; Fatemi, S.; Vatani, A. *Iran. J. Chem. Chem. Eng.* **2009**, *28*, 25-44.
68. Yang, R. T. *Gas Separation by Adsorption Processes*; Butterworths: Boston, MA, USA, 1987.
69. Wakao, N.; Smith, J. M. *Chem. Eng. Sci.* **1962**, *17*, 825-834.
70. Wakao, N.; Funazkri, T. *Chem. Eng. Sci.* **1978**, *33*, 1375-1384.
71. Gupta, S. S.; Bhattacharyya, K. G. *Adv. Colloid. Interface.* **2011**, *162*, 39-58.
72. Lagergren, S. *Handlingar.* **1898**, *24*, 1-39.
73. Ho, Y. S.; McKay, G. *Process. Saf. Environ. Protect.* **1998**, *76*, 183-191.
74. Marczewski, A. W. *Langmuir* **2010**, *26*, 15229-15238.
75. Wan Ngah, W. S.; Hanafiah, M. A.; Yong, S. S. *Colloids. Surf. B Biointerfaces* **2008**, *65*, 18-24.
76. Ho, Y. S. *J. Hazard. Mater.* **2006**, *136*, 681-689.
77. Sampranpiboon, P.; Feng, X. *International Journal of Advances in Chemical Engineering and Biological Sciences* **2016**, *3*, 66-71.
78. Ho, Y. S.; McKay, G. *Adsorpt. Sci. Technol.* **2002**, *20*, 797-815.
79. Georgiev, D., Bogdanov, B.; Hristov, Y.; Markovska, I. *Int. J. Environ Chem. Ecological. Geological. Geophysical. Eng.* **2012**, *6*, 214-218.
80. Sparks, D. L. *Kinetics of Soil Chemical Processes*; Academic Press: San Diego, CA, USA, 1989.
81. Nibou, D.; Mekatel, H.; Amokrane, S.; Barkat, M.; Trari, M. *J. Hazard. Mater.* **2010**, *173*, 637-646.
82. Sprynskyy, M. *J. Hazard. Mater.* **2009**, *161*, 1377-1383.
83. Uslu, G.; Tanyol, M. *J. Hazard Mater.* **2006**, *135*, 87-93.
84. Khan, M. A.; Kim, S. W.; Rao, R. A. K.; Abou-Shanab, R. A. I.; Bhatnagar, A.; Song, H.; Jeon, B. H. *J. Hazard. Mater.* **2010**, *178*, 963-972.
85. Venkatraman, B. R.; Hema, K.; Nandhakumar, V.; Arivoli, S. *J. Chem. Pharm. Res.* **2011**, 3, 637-649.
86. Rahmani, A.; Zavvar Mousavi, H.; Fazli, M. *Desalination* **2010**, *253*, 94-100.